Available online at www.sciencedirect.com

SCIENCE DIRECT®

Journal of volcanology and geothermal research

ELSEVIER

Journal of Volcanology and Geothermal Research 137 (2004) 93–108

www.elsevier.com/locate/jvolgeores

# Propagation of acoustic waves in a viscoelastic two-phase system: influence of gas bubble concentration

Emanuele Marchetti[a,*], Mie Ichihara[b], Maurizio Ripepe[a]

[a] *Dipartimento di Scienze della Terra, Universita' degli Studi di Firenze, via La Pira 4, 50121 Florence, Italy*
[b] *Earthquake Research Institute, University of Tokyo Yayoi 1-1-1, Bunkyo, Tokyo, 113-0032, Japan*

**Abstract**

Volcanic explosions generate pressure perturbations in the atmosphere and a seismic wavefield in the ground. The source is therefore well coupled with the atmosphere and the ground. The acoustic and elastic wavefields reflect dynamical processes at the source and the viscoelastic properties of the magma–gas medium. At low pressure (< 10 MPa), magma cannot be considered as a homogeneous medium, and must be treated as a mixture of fluid magma and gas bubbles. Acoustic waves are strongly affected by the transmission properties of the magma–gas medium. We analyze the propagation of the acoustic wavefield in a two-phase medium in which the viscosity and compressibility are spatially inhomogeneous. Gas bubble nucleation starts when the magma pressure drops below the supersaturation level (at a depth of a few hundred m for $H_2O$ in basaltic magmas) and the gas-volume fraction increases toward the surface, reaching its maximum value at the magma–air interface. The variation of gas-volume fraction is non-linear with depth and is particularly strong at shallow depths (< 50 m). Density and sound velocity of the mixture drop drastically and the shear viscosity of the mixture increases with decreasing depth. Under these conditions, we tested if the propagation of an acoustic wavefield generated by a source embedded in the magma column can generate an infrasonic wavefield in the atmosphere. The acoustic wavefield in the magma is here modeled as function of the void fraction in the magma and resonance is considered to be induced only by body-wave. Large gas bubble concentrations (>70%) strongly affect the propagation properties of the acoustic wavefield. We found that the amplitude of the infrasonic wavefield in the atmosphere typically recorded in case of strombolian explosions ($2 \times 10^5$ Pa) can be explained by a deep (>50 m) source embedded in the magma conduit only if a very large unrealistic pressure drop ($10^{13}$ Pa) is assumed. The strong damping, linked to the poor elastic properties of the shallow magma–gas mixture, prevents the efficient propagation of the acoustic waves in the magma–gas mixture, and resonance of body waves cannot occur. Infrasonic waves can be transmitted from the magma to the atmosphere only when the source is very shallow (< 10 m). In conclusion, we neglect the possibility that resonance of body waves can induce infrasonic waves in the atmosphere. Moreover, we introduce new evidence of a strong attenuation induced by the shear viscosity on the propagation of elastic waves in a gas-rich magma. We believe that this latter result could have also a large impact on all the theories based on the resonance of elastic waves in a conduit as model to explain tremor and/or LP events on volcanoes.


*Keywords:* gas bubbles; viscoelasticity; wave propagation; resonance

* Corresponding author.
*E-mail addresses:* marchetti@geo.unifi.it (E. Marchetti), ichihara@eri.u-tokyo.ac.jp (M. Ichihara), mripepe@geo.unifi.it (M. Ripepe).

0377-0273/$ - see front matter © 2004 Elsevier B.V. All rights reserved.
doi:10.1016/j.jvolgeores.2004.05.002

## 1. Introduction

Seismic and acoustic waves produced by volcanic explosions are usually explained in terms of (1) source dynamics or (2) resonance properties of the source volume. The former models relate the acoustic wavefield to the explosion of a gas bubble near the surface of the magma column (Vergniolle and Brandeis, 1996; Ripepe et al., 1996). In the resonance models, a sudden pressure drop embedded in, or at the top of the magma column (Chouet, 1985; Buckingham and Garces, 1996; Neuberg, 2000) generates body and interface waves trapped in the magma body. Acoustic resonance in the magma–gas fluid is believed to enhance the energy content of the source, which in this way can radiate acoustic waves in the atmosphere as infrasound (Buckingham and Garces, 1996) and in the ground as seismic signals (Chouet, 1985; Neuberg, 2000). The radiated energy depends on the impedance contrast at the magma–air and magma–conduit wall boundaries. Resonance models are based on strong agreement between measured and theoretical wavefields. The latter is calculated by taking into consideration the propagation of acoustic waves in the viscoelastic magma–gas medium. The role played by gas has always been considered as a fundamental factor affecting the elastic properties of the melt. Models developed so far however have generally neglected the viscoelastic effects of the void fraction on acoustic propagation. In this paper, we analyze the acoustic wavefield in terms of propagation of viscoelastic wave in a two-phase medium. This problem has been developed by other authors before us to explain both infrasonic waves (Garces et al., 2000) and volcanic tremor (Chouet, 1985; Neuberg, 2000; Neuberg et al., 2000), but always without considering the attenuation induced by the large viscosity changes due to the bubbles in the melt.

At low pressure ($<10^7$ Pa), the magma cannot be considered as a homogeneous medium, but must be treated as a mixture of fluid magma and gas bubbles. Overpressure in gas bubbles is considered critical in triggering volcanic explosions. Many theoretical (Sparks, 1978; Toramaru, 1989) and experimental studies (Lyakhovsky et al., 1996; Navon et al., 1998) focus on the nucleation and growth of bubbles in magma. Nucleation starts when the pressure in the volcanic conduit drops below the supersaturation level, which corresponds to a depth of a few hundred meters for $H_2O$ in basaltic magma (Sparks, 1978). The void fraction increases from the nucleation depth toward the surface, and reaches its maximum value at the magma–air interface. The void fraction profile is non-linear with depth and the gas bubble content is particularly high near the surface. As a consequence the seismo-acoustic properties of the melt change significantly with the decrease of depth (Massol and Jaupart, 1999; Garces et al., 2000). The increase in void fraction induces a drop in density and sound velocity of the mixture (Aki et al., 1978; Chouet, 1996) and a significant increase in the mixture viscosity (Jaupart and Vergniolle, 1989). In order to understand if the infrasonic wavefield generated by volcanic explosions can be explained in terms of propagation of an elastic wavefield induced by an embedded source and transmission to the atmosphere (Buckingham and Garces, 1996), we investigate the propagation of an acoustic wave in the shallow ($<200$ m) bubbly section of the volcanic conduit. We calculate the attenuation of the acoustic wavefield generated by a source embedded in the magma column as a function of the void fraction of the melt. Laboratory experiments suggest a large attenuation of pressure waves in viscoelastic bubbly liquids with a viscosity in the order of $10^3$ Pa s (Ichihara et al., 2004). This paper presents new insights on viscoelastic effects in the propagation of acoustic waves in a bubbly magma.

## 2. Shallow volcanic system

The propagation of an acoustic wave in a shallow volcanic system ($<1$ km) is controlled by the presence of gas bubbles and minerals, which vary the rheology of the melt. The void fraction is a critical parameter, because it affects the viscosity, density and sound speed of the mixture. When the amount of gas is sufficiently high (>70%) and the bubbles are in contact with each other (foam), the physical properties of the system depart from pure elastic behavior and are controlled by the surface tension of the bubbles (Cashman and Mangan, 1994; Proussevitch et al., 1993). It is therefore necessary to analyze the magmatic system as a multiphase mixture. In this study, we neglect the presence of minerals and consider the

shallow magma as a mixture of silicate melt and exsolved gas bubbles. This assumption simplifies the model without reducing its reliability. The presence of minerals mainly affects the viscosity of the melt. A melt with a higher percentage of minerals is more viscous (Saar et al., 2001). The nucleation of bubbles and crystallisation of minerals are linked in a magmatic system and both lead to analogous changes in the viscosity of the mixture (Sparks et al., 1994; Spera, 1999). Therefore, neglecting the effects of minerals in our model will lead to an underestimation of the actual viscosity of the magmatic system.

## 3. Void fraction and exsolution model

The distribution of voids with depth in the volcanic conduit is based on the assumption that the volcanic conduit is open. In open conduit volcanoes (e.g., Stromboli, Etna) infrasonic records reveal a persistent degassing activity associated with volcanic tremor (Ripepe et al., 1996, 2001b). Individual pressure pulses repeat regularly in time (at a rate ~ 1 s) and can be explained by the bursting of small gas bubbles at the top of the magma column (Ripepe and Gordeev, 1999). This persistent bursting of small gas bubble at the top of the magma column will prevent the establishment of a large overpressure and ensures a nearly hydrostatic pressure profile.

The steady eruptive style and persistent degassing activity observed on open conduit volcanoes suggests a continuous supply of fresh magma (Kazahaya et al., 1994; Stevenson and Blake, 1998). We consider that gas bubble nucleation starts at the exsolution depth, which is mainly controlled by the type and concentration of the gaseous phase. For example, considering water and carbon dioxide as the only two volatiles dissolved in the magma, we can estimate two different exsolution levels. Although the $CO_2$ concentration is much smaller than that of $H_2O$ in magma, the exsolution level of $CO_2$ is deeper than that of $H_2O$ in most cases. This is a result of the solubility of the two gas phases, which is much higher for $H_2O$ than for $CO_2$. In a mafic magma, the solubility of $H_2O$ is obtained as a function of hydrostatic pressure $P$ (Hamilton et al., 1964) as:

$$x_{H_2O} = K_{H_2O} P^{0.7}, \quad (1)$$

where $x_{H_2O}$ in weight fraction of $H_2O$, $P$ is pressure (Pa) and $K_{H_2O} = 6.8 \times 10^{-8}$ wt.%/Pa$^{0.7}$ is an experimental parameter. The solubility of $CO_2$ is obtained as (Stolper and Holloway, 1988):

$$x_{CO_2} = K_{CO_2} P, \quad (2)$$

where $x_{CO_2}$ in weight fraction of $CO_2$, $P$ is pressure (Pa) and $K_{CO_2} = 4.4 \times 10^{-12}$ wt.%/Pa is an experimental parameter.

Some exsolution models consider $CO_2$ bubbles between the exsolution depths of $CO_2$ and $H_2O$, and the coexistence of the two gas phases above the $H_2O$ exsolution depth. Actually, a system containing two volatiles behaves in a slightly different way from a system containing a single volatile (Tait et al., 1989). When the concentration of one of the volatiles exceeds the solubility limit, both the volatiles exsolve with different partial pressures as functions of the initial concentrations, according to Henry's law, as expressed by Eqs. (1) and (2), above. Accordingly, at a depth of ~1000 m, where the pressure is higher than the $H_2O$ supersaturation pressure, the exsolution of $CO_2$ will also force some $H_2O$ to exsolve. This is true for all gaseous phases in general. In the specific case addressed here, the great difference in solubility between $H_2O$ and $CO_2$ tends to strongly limit such process.

In this paper we assume $H_2O$ as the only volatile dissolved in the melt. In open conduit volcanic systems like Stromboli, where the volume of $H_2O$ is three times larger than that of $CO_2$ (Allard et al., 1994), this approximation is quite close to reality. Considering an initial $H_2O$ concentration of 0.35 wt.% dissolved in the basaltic magma (Pineau and Javoy, 1994; Sparks et al., 1994), a nucleation pressure $P_o \sim 5 \times 10^6$ Pa is obtained from Eq. (1). When the magma is decompressed to atmospheric pressure, $P_{atm} = 10^5$ Pa, the initial 0.35 wt.% of the volatile dissolved in the melt reduces to 0.02 wt.%. If all the gas phase remains in the magma (assuming a closed system), the void fraction may exceed 98%, far larger than the 75% generally considered as the fragmentation limit.

In open conduit volcanic systems fragmentation will not be reached and the void fraction near the magma surface can be estimated from the density of scoria ejected during explosions. In the present paper, we assume a void fraction at the free surface of the magma column of 44%, as this value has been

estimated for Stromboli Volcano, which is the typical example of open conduit volcanic system. This indicates that the system is open and that bubbles are free to leave the melt. This is evidenced by the strong degassing of the magmatic system at Stromboli and indicates that the bubbles rise much faster than the magma, which can be considered stationery compared to the bubble rise speed.

The distribution of voids in the conduit is determined by the upward motion of the magma, volatile exsolution and bubble degassing. Mathematical models describing such conduit flows have been studied by various authors (Melnik and Sparks, 1999; Yoshida and Koyaguchi, 1999; Dobran, 1992). Most of these models are intended for silicic magma flow, which may cause Plinian eruptions. The constitutive equations for a basaltic system may be different from those used in these models. Determining the precise void distribution is not the purpose of the present work. The effects of bubble motion relative to melt on the void fraction distribution will be analyzed in a future paper. For our present purpose, we represent the void distribution as a simple function, which increases as pressure decreases according to:

$$\phi = \phi_o \left( \frac{P_o - P}{P_o - P_{atm}} \right)^n, \tag{3}$$

where $P_o$ is the nucleation pressure, $P$ is the local pressure, $P_{atm}$ is the atmospheric pressure, $\phi$ is the void fraction distribution, $\phi_o = 0.44$ is the void fraction at the magma surface and $n$ is an arbitrary parameter. We assume $n = 1$.

## 4. Physical property of the system

Gas bubbles in the melt significantly affect the seismo-acoustic properties of the liquid–gas mixture. An increase in void fraction causes a decrease of the two-phase medium density ($\rho$):

$$\rho = \rho_g \phi + \rho_m (1 - \phi), \tag{4}$$

where $\rho_m$ and $\rho_g$ are the densities of the melt and gas, respectively. We assume a melt density of 2700 kg/m$^3$. The gas density is obtained from the perfect gas law as:

$$\rho_g = \frac{P}{R_g T}, \tag{5}$$

where the gas constant $R_g = 8.31/0.018$ J/kg/K for $H_2O$ and the temperature $T$ is taken as 1200 K. The pressure profile is fixed by the magmastatic relation:

$$\frac{dP}{dz} = \rho g, \tag{6}$$

where $z$ is the vertical coordinate, taken positive downward, and $g$ is the gravitational acceleration. Solution of Eqs. (3)–(6) yields the void fraction and

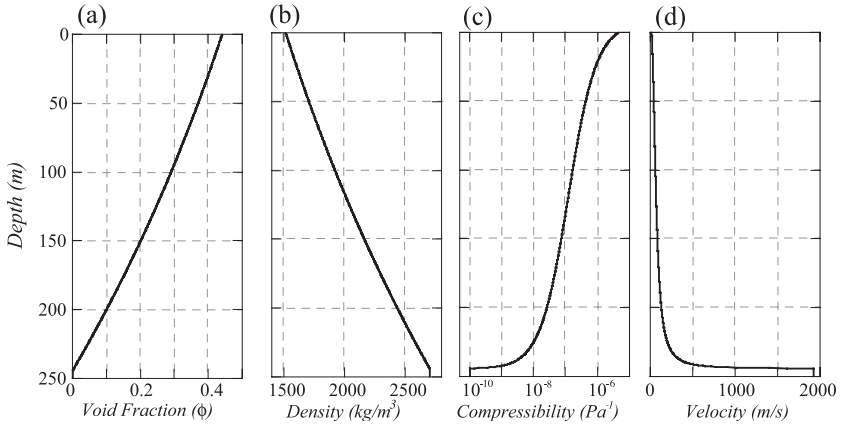


Fig. 1. (a) Void fraction of the magma–gas mixture as a function of depth in the conduit. Physical properties of the two-phase medium in the volcanic conduit: density (b), compressibility (c) and longitudinal wave propagation velocity (d).

density as functions of depth (Fig. 1a and b). Once the void fraction and pressure profiles are known, the acoustic properties of the system are known as a function of depth in the conduit (Fig. 1c–d). The compressibility, $k$, increases with the void fraction as:

$$k = k_g\phi + k_m(1-\phi) \quad (7)$$

where $k_m$ and $k_g$ represent the magma compressibility and gas compressibility, respectively. We assume $k_m = 10^{-10}$ Pa$^{-1}$ for a sound velocity of 2000 m/s in pure melt (Murase and McBirney, 1973) and fix $k_g = P^{-1}$ for constant temperature (Eq. (5)). The decrease in density and compressibility of the mixture affects the sound velocity $c$ of the system according to the relation:

$$c = 1/\sqrt{e^k}. \quad (8)$$

The sound velocity in the magma–gas mixture decreases drastically with the increase in gas bubble concentration (Fig. 1d). The minimum velocity of the two-phase system is much lower ($\sim$ 20 m/s) than the sound velocity of either the magma or steam (Gibson, 1970; Kieffer, 1977). Note that Eq. (8) defines the sound speed at the equilibrium. In low-viscosity liquids, the observed speed or the phase velocity agrees with the equilibrium values. However, recent experimental studies showed that the presence of bubbles in high-viscosity liquids ($\eta \sim 10^3$ Pa s) reduces the sound velocity in the mixture, but the effect is not so critical as theoretically predicted (Ichihara et al., 2004; Ichihara and Kameda, 2004-this issue). The equations of sound velocity in bubbly liquid are indeed derived for low-viscosity liquids, and their applicability to high-viscosity liquids is not trivial. In the present study, we apply equations of the sound speed derived for low-viscosity liquids. Future improvement of the model will consider the proper sound velocity in high-viscosity ($\eta \sim 10^3$ Pa s) bubbly magma. The viscosity of the system is another critical parameter that is strongly affected by void fraction. We assume that the mixture of silicate melt and bubbles is an isotropic linear viscous medium with rheology represented by the two parameters, shear and bulk viscosity. The viscoelastic nature of the pure silicate melt (Webb, 1997) is neglected, because the relaxation time for basaltic magma has a time scale $< 10^{-5}$ s (Dingwell and Webb, 1989), which is much shorter than the time scale of acoustic waves ($>5 \times 10^{-2}$ s). Both the shear and bulk viscosity are controlled by the void fraction and both increase with the gas-volume fraction via two different processes, namely a decrease in dissolved $H_2O$ (Jaupart, 1996; Massol and Jaupart, 1999) on the one hand and an increase in the number of undeformable gas bubble on the other hand. The decrease in dissolved $H_2O$ is not compensated by the fluidizing role of the bubbles (Richet et al., 1996). Undeformable bubbles increase the shear viscosity $\eta_s$ of the mixture according to the relation:

$$\eta_s(\phi) = \eta_{so}\left(1 - \frac{\phi}{\phi_c}\right)^{-5/2} \quad (9)$$

where $\eta_{so}$ is the shear viscosity of the melt in the absence of bubbles and $\phi_c = 0.6$ is a model parameter (Spera, 1999). Eq. (9) is valid for bubbles with small values of the capillary index $C_a$:

$$C_a = \frac{\dot{\epsilon}\eta_{so}R}{\sigma}, \quad (10)$$

where $\dot{\epsilon}$ is the shear rate, $R$ is the bubble radius and $s$ is the surface tension of the melt vapor.

The capillary index represents the ratio between viscous forces ($\dot{\epsilon}\eta_{so}$) and tension at the gas–melt surface ($\sigma/R$). This ratio is difficult to estimate. Notice, however, that $\dot{\epsilon}\eta_{so}$ tends to deform the bubble, while $\sigma/R$ tends to keep the bubble spherical. Therefore, a convenient way to estimate $C_a$ it is to consider the shape of the bubbles (Stein and Spera, 1992); $C_a = 0$ for perfectly spherical bubbles, while bubble elongation is significant when $C_a$ tends to 1. The explosive activity associated with open conduit volcanic system is generally consistent with scoria containing bubbles populations that are quite spherical, which suggests a capillary index less than unity.

The shear viscosity $\eta_s$ of the magma–gas mixture changes with the void fraction according to Eq. (9). At the same time, the exsolution of water from the melt according to Eq. (1) induces a change in the shear viscosity of the melt $\eta_{so}$. In order to estimate the shear viscosity of residual melt, produced by gas bubbles exsolution, we apply the equation developed by Shaw

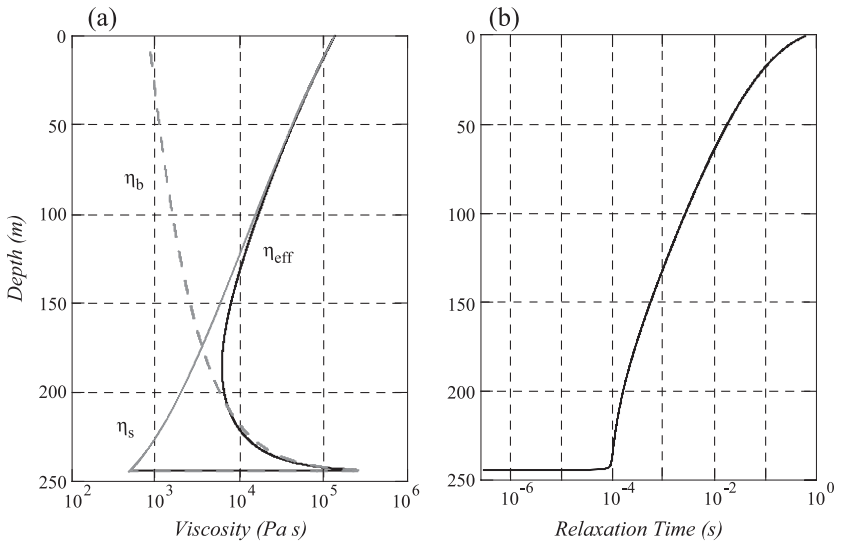


Fig. 2. Viscosity of the magma–gas mixture in the volcanic conduit. The shear viscosity $\eta_s$ of the mixture (gray line) increases with the void fraction. The bulk viscosity $\eta_b$ (dashed gray line) undergoes a sharp increase at the exsolution depth. As a consequence, the effective viscosity of the mixture $\eta_{eff}$ (black line) increases with void fraction after an initial peak at the exsolution level (a). Relaxation time evaluated for the magma gas mixture (b).

(1972) assuming the composition of basaltic magma and scorias, which we infer representative of the residual melt before and after water exsolution. In the present model, we take into consideration the compositions derived for Stromboli Volcano (Francalanci et al., 1993). As a consequence, we assume in the present paper a shear viscosity of the melt $\eta_{so} = 500$ Pa s before the exsolution of bubbles and $\eta_{so} = 5000$ Pa s at the free surface. Shaw's model indicates that the shear viscosity depends on the amount of dissolved water almost linearly in the present range of change. Therefore, we assume, between $\eta_{so} = 500$ and 5000 Pa s, that the shear viscosity changes proportional to $P^{0.7}$ as in Eq. (1).

The void fraction affects the bulk viscosity of the mixture in a similar way. Based on the formulation of Ichihara and Kameda (2004-this issue), and considering that gas has a larger compressibility than the melt ($k_g \gg k_m$), the bulk viscosity ($\eta_b$) of the mixture is given by:

$$\eta_b(\phi) = \frac{1-\phi}{(\phi + k_m/k_g)^2}\left[\frac{4}{3}\eta_{so}\phi + \eta_{bo}\left(\frac{k_m}{k_g}\right)^2\right]. \quad (11)$$

As for general fluids (Landau and Lifshitz, 1987), we may use $\eta_{bo} = \eta_{so}$, so that Eq. (11) can be simplified as:

$$\eta_b(\phi) = \frac{4}{3}\eta_{so}\frac{1-\phi}{\phi}, \ (\phi \gg k_m/k_g), \quad (12)$$

$$\eta_b(\phi) = \eta_{so}(1-\phi) \times \left[\frac{4}{3}\phi\left(\frac{k_g}{k_m}\right)^2 + 1\right], (\phi \ll k_m/k_g). \quad (13)$$

Note that Eq. (12) agrees with the expression used by Massol and Jaupart (1999) for large void fraction. The bulk viscosity of the mixture $\eta_b$ shows a sharp increase for low values of void fraction and decreases when the compressibility of the mixture becomes larger as the number of gas bubbles increases. As a consequence, the presence of bubbles causes a net increase in medium viscosity (Fig. 2). The bulk viscosity increases mainly at low void fraction ($\phi < 5 \times 10^{-4}$), while the shear viscosity increases towards the surface, where the bubble content is higher (Fig. 2).

## 5. Attenuation of the medium

Acoustic wave absorption in a fluid depends on the time lag occurring between the stress and the strain. Attenuation in a bubbly-liquid with low gas-volume fraction, up to a few percent, is related to viscosity, heat transfer and acoustic radiation.

To formulate the relationship between stress and strain, we consider the general equation of motion for one-dimensional flow:

$$\rho\frac{\partial^2 u_z}{\partial t^2} = -\frac{\partial p}{\partial z} + \frac{\partial D_{zz}}{\partial z} + \frac{\partial D_{zx}}{\partial x} + \frac{\partial D_{zy}}{\partial y}, \tag{14}$$

where $u_z$ is the vertical displacement, $D_{zi}$ ($i=x,y,z$) are the components of the deviatoric stress tensor and $p$ is the pressure. Averaging Eq. (14) over the horizontal cross section of the conduit, we obtain:

$$\rho\frac{\partial^2 u}{\partial t^2} = -\frac{\partial p}{\partial z} + \frac{\partial D}{\partial z} - Q_w. \tag{15}$$

This equation represents the averaged vertical displacement u as a function of pressure $p$, averaged normal component of the deviatoric stress D and wall friction force per unit volume $Q_w$, obtained from the term $\frac{\partial D_{zx}}{\partial x} + \frac{\partial D_{zy}}{\partial y}$ in Eq. (14).

The relation between pressure and strain for an attenuating medium is expressed by Stokes equation:

$$p(z,t) = \rho c^2 s + \eta_b\frac{\partial s}{\partial t}, \tag{16}$$

where $s$ is the variable which represents the strain in the medium. Rarefaction and compression, associated with the pressure wave propagation, cause a change in the local value of density ($\rho$):

$$s = \frac{\rho - \rho_o}{\rho_o}, \tag{17}$$

where $\rho_o$ is the mean density. Considering a plane wave and assuming small displacements producing small density variations, the strain in the medium can be expressed as:

$$s = -\frac{\partial u(z,t)}{\partial z}, \tag{18}$$

where $u(z,t)$ is the displacement of the medium. Substituting (18) into Eq. (16), the pressure is given by:

$$p(z,t) = -\rho c^2\frac{\partial u(z,t)}{\partial z} - \eta_b\frac{\partial^2 u(z,t)}{\partial t\partial z}. \tag{19}$$

The deviatoric stress tensor $D_{ij}$ is related to the shear viscosity and non-volumetric strain rate by:

$$D_{ij} = \eta_s\left(\frac{\partial^2 u_i}{\partial t\partial x_j} + \frac{\partial^2 u_j}{\partial t\partial x_i} - \frac{2}{3}\delta_{ij}\frac{\partial^2 u_k}{\partial t\partial x_k}\right). \tag{20}$$

where $\delta_{ij}$ is Kronecker's delta. According to Eq. (20):

$$D = \frac{4}{3}\eta_s\frac{\partial^2 u}{\partial t\partial z}. \tag{21}$$

The effect of wall friction on transient one-dimensional laminar pipe flow has been formulated by Achard and Lespinard (1981), who obtained the following relation between the wall friction force per unit volume ($Q_w$) and mean velocity ($v$) as a good approximation for low-frequency waves:

$$Q_w + \xi\frac{dQ_w}{dt} = \frac{8\eta_s}{a^2}\left(1 + \frac{3}{2}\xi\frac{d}{dt}\right)v, \tag{22}$$

where $a$ is the conduit radius and $\xi = 0.0833\rho a^2/\eta_s$. Although the present application is different from the model considered by Achard and Lespinard (1981) in that our flow is compressible and the mean velocity varies along the conduit axis, we assume that Eq. (22) is locally valid, so that:

$$Q_w + \xi\frac{\partial Q_w}{\partial t} = \frac{8\eta_s}{a^2}\left(1 + \frac{3}{2}\xi\frac{\partial}{\partial t}\right)\frac{\partial u(z,t)}{\partial t}. \tag{23}$$

Using Eqs. (19), (21) and (23), and assuming a solution of the form:

$$u(z,t) = X(z)e^{i\omega t}, \tag{24}$$

Eq. (15) may be rewritten as:

$$-\left(\rho - \frac{Q_\omega}{\omega^2}\right)\omega^2 X = \frac{d}{dz}\left[\left(\rho c^2 + i\frac{4}{3}\omega\eta_{eff}\right)\frac{dX}{dz}\right], \tag{25}$$

where $\eta_{\text{eff}}$ is the effective viscosity:

$$\eta_{\text{eff}} = \frac{3}{4}\eta_{\text{b}} + \eta_{\text{s}} \tag{26}$$

and

$$Q_\omega = (8\eta_{\text{s}}/a^2)i\omega\left(1 + \frac{3}{2}i\omega\xi\right)\Big/(1 + i\omega\xi) \tag{27}$$

is the wall friction force per unit length.

Because the material properties $\rho$, $c$, $\eta_{\text{eff}}$ and $\eta_{\text{s}}$ strongly depend on $z$, Eq. (25) is non-linear and can not be solved analytically. To solve this equation, we divide the conduit in a series of horizontal layers and assume that the medium is homogeneous within each layer. The following equation is valid within a single layer:

$$\frac{\mathrm{d}^2X}{\mathrm{d}z^2} = -\left(\frac{\rho - Q_\omega/\omega^2}{\rho c^2 + i\omega\frac{4}{3}\eta_{\text{eff}}}\right)\omega^2 X. \tag{28}$$

Eq. (28) has a solution of the form:

$$X(z) = Ae^{\pm ik'z}, \tag{29}$$

where

$$\frac{k'}{\omega} = \sqrt{\frac{\rho - Q\omega/\omega^2}{\rho c^2 + i\omega\frac{4}{3}\eta_{\text{eff}}}}. \tag{30}$$

Eq. (30) yields $k'$ as a complex function of $\omega$. Because the material properties depend on $z$, $k'$ also depends on $z$. Therefore, we represent $k'$ in terms of real functions of $\omega$ and $z$ as:

$$k' = k(\omega, z) - i\alpha(\omega, z) \qquad (k > 0,\ \alpha > 0). \tag{31}$$

Then, from Eqs. (24) and (29), we obtain upgoing ($u_{\text{U}}$) and downgoing ($u_{\text{D}}$) waves, whose amplitudes decrease along the wave propagation direction. The attenuation coefficient $\alpha$ is obtained from the relations:

$$u_{\text{U}}(z,t) = Ae^{\alpha(\omega,z)z}e^{i(\omega t + k(\omega,z)z)}, \tag{32}$$

$$u_{\text{D}}(z,t) = Ae^{-\alpha(\omega,z)z}e^{i(\omega t - k(\omega,z)z)}. \tag{33}$$

Fig. 3 shows the attenuation coefficient in the volcanic conduit calculated from dispersion using the parameters given in Figs. 1 and 2. The effect of the conduit wall is not considered in the results shown in Fig. 3. Attenuation is affected by many parameters. To get a better idea of the effects of each parameters, we neglect the wall friction term and transform Eq. (30) into the following approximate form:

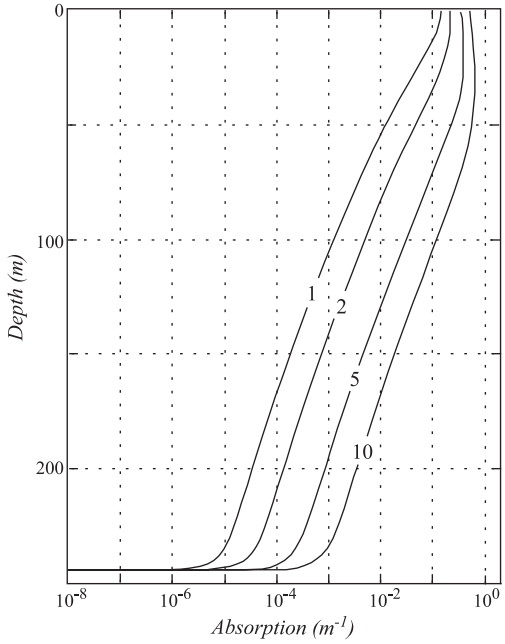


Fig. 3. Viscous attenuation coefficient in the volcanic conduit. Attenuation strongly depends on the frequency of the pressure wave. Attenuation is shown for a 1-, 2-, 5- and 10-Hz pressure wave. The effect of conduit wall is not taken into consideration.

$$k' = \frac{\omega}{c}\left(1 + i\omega\frac{4\eta_{\text{eff}}}{3\rho c^2}\right)^{-1/2} \sim \frac{\omega}{c} - i\omega^2\frac{2\eta_{\text{eff}}}{3\rho c^3}. \tag{34}$$

This approximation holds for low-frequency waves. Eq. (34) shows that attenuation efficiently increases when the velocity of the acoustic wave decreases. Viscous damping increases from the exsolution depth to the surface of the conduit because the velocity of the pressure wave and the mixture density both decrease, while the viscosity increases. The presence of gas bubbles causes a net increase in the viscous attenuation of the magma–gas mixture even for low void fraction. This behavior is linked to the sharp increase in bulk viscosity (see Fig. 2). Eq. (34) also shows that the attenuation coefficient depends on

the frequency of the acoustic wave. Viscous attenuation is larger for higher-frequency waves. An acoustic wave at a frequency of 1 Hz undergoes viscous attenuation two orders of magnitude lower than a 10-Hz acoustic wave (Fig. 3). Our present work is focused mainly on frequencies between 1 and 10 Hz, typical of the frequency content of the infrasonic wavefield associated with strombolian explosions (Vergniolle et al., 1996; Buckingham and Garces, 1996; Ripepe and Marchetti, 2002; Johnson et al., 2003). At depths below the nucleation depth, where the dense basaltic magma is without bubbles, the attenuation of a 5-Hz acoustic wave is very low ($\sim 10^{-8}$ m$^{-1}$). Attenuation increases with decreasing depth, and reaches its maximum value $>10^{-1}$ m$^{-1}$ near the free surface. At the free surface, the two-phase system is rich in gas (44%), highly viscous ($10^5$ Pa s), and has a low density ($\sim$ 1500 kg m$^{-3}$) and low sound speed (20 m/s) (Fig. 1).

The contribution of wall friction to the attenuation coefficient is calculated from Eq. (30) for several conduit radii and for an acoustic wave at a frequency of 5 Hz. These results are illustrated in Fig. 4. Comparison between Figs. 3 and 4 indicates that the effect of wall friction is indeed important for small conduit radii (<2 m), but becomes trivial for conduit radii larger than 20 m.

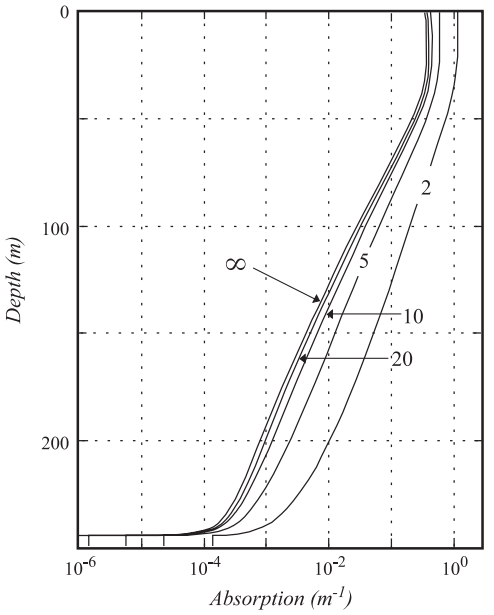


Fig. 4. Attenuation coefficient due to the friction at the wall of the volcanic conduit. The attenuation is evaluated for a 5-Hz pressure wave for different values of the conduit radius (2, 5, 10 and 20 m). Attenuation strongly decreases with the increase of conduit radius and becomes trivial for radii >20 m. The absence of friction, which corresponds to body wave propagation in an infinite half-space, is simulated assuming infinite radius of the volcanic conduit.

Our model is developed by taking into consideration a conduit with cylindrical geometry in the last 200 m, with a radius ranging between 2 and 10 m.

## 6. Acoustic scattering

The presence of gas bubbles in the melt introduces an additional component of attenuation in the bubbly fluid in the form of acoustic wave scattering. The scattering efficiency depends on the ratio of the frequency of the acoustic wave to the eigenfrequency of the bubbles. When the ratio is $\sim$ 1, the acoustic wave scattering ($\alpha_s$) is the most efficient and is given by (Kinsler and Frey, 1962):

$$\alpha_s = \frac{10^3 \pi N R^2}{2}, \tag{35}$$

where $N$ is the number of bubbles per unit volume and $R$ is the mean bubble radius. The eigenfrequency of bubble oscillation is a function of the bubble radius. An eigenfrequency of 5–10 Hz requires a bubble radius of $\sim$ 1 cm. This bubble size is larger than the bubble size (1–2 mm) usually observed in scorias at Stromboli. As a consequence, the effect of scattering is probably not so severe and this effect is neglected in the present model. Therefore, we conclude that attenuation is mainly controlled by the viscosity of the medium and by the size of the conduit.

## 7. Acoustic wave propagation in a layered two-phase medium

We analyze the propagation of an acoustic wave in the volcanic conduit by assuming that the fluid column consists of horizontal layers of magma–gas mixture. The acoustic properties within the $i$-th layer at depth $z_{i-1} < z < z_i$ are assumed to be uniform and are represented by the values obtained at $z = z_i$ (Figs. 1 and 2). The 0-th layer is the atmosphere and is represented by an infinite half space. The boundary

between the atmosphere and the magma is at $z = z_0 = 0$. An upward incident pressure wave is assumed at the bottom of the $s$-th layer at a depth $z = z_s$. The model is shown in Fig. 5.

To calculate wave propagation in this layered medium, we take in account the reflection and transmission coefficients at the boundaries between adjacent layers. We apply the mathematical method of Kennet and Kerry (1979). The original theory treats three-dimensional wave propagation in elastic layers with an elastic attenuation. For one-dimensional wave propagation in a viscous liquid, the theory is much simplified and is described in Appendix A.

The presence of gas bubbles changes the rheology of the melt, increasing the attenuation in the two-phase mixture. Many studies analyzed the attenuation of pressure waves in a bubbly liquid with low viscosity (Commander and Prosperetti, 1989; Prosperetti, 1984). Using the model of Commander and Prosperetti (1989), for example, Chouet (1996) predicts attenuation $\sim 10^{-5}$–$10^{-7}$ dB/cm for a basaltic magma, assuming a temperature of 1100 °C, depths of 100–1000 m, magma viscosity of 10 Pa s and a 1% void fraction of bubbles with radii 0.3–3 mm. These analyses take account attenuation due only to effective bulk viscosity. However, laboratory experiments performed on high-viscosity liquids show different results, mainly because the contribution of shear viscosity on the attenuation of viscoelastic waves is considerable (Fig. 2). Laboratory experiments point to severe attenuation of shock and pressure waves in high-viscosity liquids ($\eta \sim 10^3$ Pa s) containing bubbles (Ichihara et al., 2004), even for a void fraction as low as 1%. In this case, velocity and attenuation of pressure wave strongly depend on shear modulus and shear viscosity (Ichihara et al., 2004; Ichihara and Kameda, 2004-this issue).

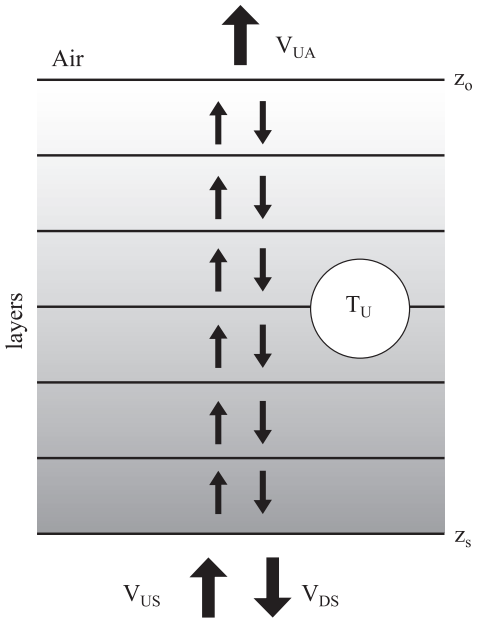


Fig. 5. Sketch of the magma–gas mixture layers used in our analysis of acoustic wave propagation.

Strombolian explosions (e.g., at Stromboli, Etna, Erebus, Karymsky) produce pressure perturbations in the atmosphere on the order of $10^5$ Pa at the vent (Vergniolle and Brandeis, 1996; Ripepe et al., 2001a,b; Johnson et al., 2003). Considering this value, we calculate which pressure drop we should need at different depth of the source in the magma column to generate a pressure of $10^5$ Pa in the atmosphere. Based on the frequency content of the recorded acoustic signal, we consider a pressure wave at a frequency of 5 Hz. Fig. 6 shows that higher frequencies and narrower conduits require larger pressures at the source in order to produce a pressure of $10^5$ Pa at the surface. For a 5-Hz pressure wave and a conduit radius of 5 m, a pressure pulse of $10^5$ Pa at the free surface requires (1) a very shallow (<2 m) position of the source with source pressure of $<10^7$ Pa or (2) a deeper more energetic pressure source $>3 \times 10^7$ Pa (Fig. 6). The attenuation effect is more severe if we consider a narrower (<5 m) conduit. For a larger conduit radius (>10 m), the attenuation due to frictional effects at the conduit wall is weak (Fig. 4); however, the source still needs to be shallower than 10–15 m to produce the observed pressure amplitude at the free surface unless this source is extremely strong, with a pressure larger than $10^9$ Pa (Fig. 6). Buckingham and Garces (1996) modelled the acoustic wave associated with explosions at Stromboli in terms of pressure wave propagation induced by a strong pressure source ($10^9$ Pa) deep embedded in the magma (80 m) conduit and explained the observed acoustic spectrum in terms of wave resonance in the conduit. According to our model, a deep (80 m) source can produce a $10^5$ Pa infrasonic wave in the atmosphere only assuming a pressure drop at the source of $10^{13}$ Pa, which is much stronger than what

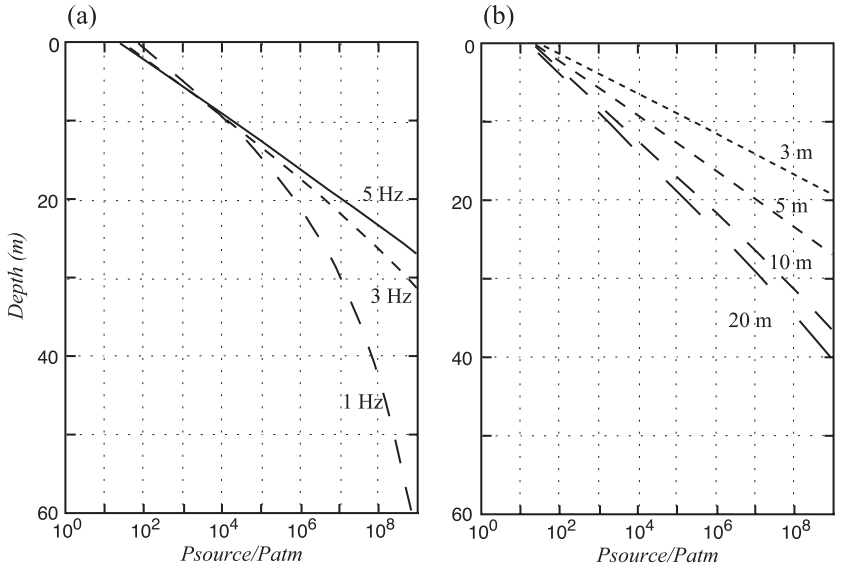


Fig. 6. Amplitude of the pressure perturbation (expressed as $P_{source}/P_{atm}$) in the conduit. The pressure at the source is evaluated in order to produce a pressure onset similar to explosions at Stromboli ($P \sim 10^5$ Pa). Pressure source as a function of depth in the conduit taking into consideration a pressure wave at frequencies of 1, 3 and 5 Hz, which propagates in a 5-m radius volcanic conduit (a), and a 5-Hz pressure wave, which propagates in a volcanic conduit with radii of 3, 5, 10 and 20 m (b).

predicted by Buckingham and Garces (1996). Moreover, the strong viscoelastic attenuation, in the shallowest portion of the volcanic conduit, will prevent the wave to travel downward the magma column and will not allow the resonance of the body wave in the conduit.

In our model, infrasonic waves with $P \sim 10^5$ Pa and resonance of the magma column can be possible only by reducing of several orders of magnitude the effective viscosity $\eta_{eff}$ in the uppermost part of the fluid column (Garces et al., 2000). The relaxation time in a viscoelastic medium such as a vesicular magma is given by $\tau=(4/3)\eta_{eff}/(\rho c^2)$ (Garces, 1997). When $\tau$ is larger than the time scale of the propagating acoustic wave ($\omega^{-1}$), the medium behaves like an elastic solid and the effective viscosity decrease with $\tau\omega>1$. Our relaxation time ($\sim 0.8$ s) is larger than the time scale (0.2 s) of a 5-Hz acoustic signal, suggesting that our medium may behave like an elastic solid. However, the reduced viscosity is accompanied by an increase of the elastic modulus and associated increase in the sound speed (Bagdassarov and Dingwell, 1993; Garces et al., 2000). The increase of the sound speed increases the magma–air acoustic impedance contrast, effectively reducing the amount of acoustic energy transmitted in the atmosphere. Such effect further decreases the amplitude of the infrasonic wave to the value of $\sim 10^{-3}$ Pa, which is below the sensitivity of any infrasonic instrument.

In conclusion, the large attenuation of the viscoelastic gas-rich magma indicates that the infrasonic wavefield propagating in the atmosphere associated with strombolian explosions can not be produced by the resonance of a pressure wave in the volcanic conduit.

## 8. Conclusions

The seismo-acoustic wavefield recorded during volcanic activity is generated inside the magma conduit. The large seismo-acoustic energy measured on active volcanoes indicates that source is well coupled with the atmosphere as well as with the ground. The origin of both wavefields is still debated. Independently from the dynamics of the source, it is obvious that the source within the magma generates a pressure front that excites the magma column. Several models have suggested that the seismic and acoustic wavefields may be strongly controlled by acoustic resonance in the conduit (e.g., Chouet, 1985; Julian, 1994; Buck-

ingham and Garces, 1996). Longitudinal and radial resonance requires that acoustic waves, freely propagating along the magma column, are reflected by sharp vertical and horizontal boundaries. Vertical boundaries are identified as the free surface at the top and the nucleation depth at the bottom of the magma column, while the conduit wall provides the horizontal boundary. It is clear that resonance models require a detailed analysis of the wave propagation in the magma to explain both seismic (e.g., Chouet, 1985) and acoustic (Garces et al., 2000) waves. However, previous studies, aware of the importance of the viscous properties of the magma–gas mixture (e.g., Chouet, 1985; Garces et al., 2000; Neuberg et al., 2000), have mainly focused their analysis on the elastic properties of medium.

The contribution of our work is to analyze the propagation of the acoustic wavefield considering the viscoelasticity of the two-phase magma–gas mixture. At shallow depths the volatiles are no more stable as dissolved species in the melt. Gas bubbles nucleate at some depth and the void fraction increases toward the surface. The gas bubbles change the acoustic properties of the magma–gas mixture. The increase in void fraction causes a decrease in the density, bulk modulus and sound velocity of the mixture, and increases the viscosity of the two-phase fluid. These processes are non-linear with depth and lead to a strong damping of the waves near the surface (depth < 20 m).

In order to understand if the acoustic wavefield in the atmosphere associated with volcanic explosions can be explained in terms of pressure wave propagation in the conduit induced by an embedded pressure source (Buckingham and Garces, 1996), we have quantified the transmission of a pressure wavefield in a stratified viscoelastic magma–gas mixture for different source depths. Considering that explosions generally release a pressure perturbation on the order of $10^5$ Pa in the atmosphere, we calculated the required pressure at the source ($P_{source}$) as function of depth. The $P_{source}/P_{atm}$ ratio rapidly increases with increasing source depth in the magma column (Fig. 6). At a depth of 10 m, this ratio suggests a pressure at the source $>10^8$–$10^9$ Pa, taking into account a 5-Hz pressure wave and a conduit radius of 5 m. Acoustic wave amplitude is strongly reduced by the high effective viscosity ($\sim 10^5$ Pa s) of the void-rich fraction ($\sim 0.44$) in the top few meters of the magma–gas mixture. We demonstrated that attenuation also depends on the conduit wall friction and increases with decreasing conduit radius. For conduit radii larger than 10 m, attenuation by wall friction is low. Viscoelasticity has a large effect on the attenuation of acoustic waves at frequencies above 1 Hz. For a high-viscosity magma–gas mixture ($\eta_{eff} \sim 10^5$ Pa s for $\phi \sim 0.44$), we infer that wave propagation becomes effective only when the conduit is larger than 10 m, the source is shallower than 20 m and the frequency of the acoustic wave is lower than 2 Hz. Under these conditions, an acoustic wave can travel a significant distance along the conduit. However, taking into account the frequency content of the infrasonic wavefield commonly recorded on open conduit explosive volcanoes (1–10 Hz), viscous attenuation in the magma–gas medium strongly prevents the propagation of acoustic waves in the magma conduit. According to our model, the infrasonic wavefield in the atmosphere produced by strombolian explosions can be explained in terms of conduit resonance only if the source is located near the surface (in the last 10 m of the magma column). Sources embedded in the magma column at depth larger than 50 m will require pressure drop larger than $10^{13}$ Pa. This pressure drop is by far too large. Recent seismological evidence (Chouet et al., 2003) that explosions at Stromboli are triggered by a pressure drop of $10^7$ Pa at 220–260 m depth below the crater terrace. As a consequence, resonance models, based on body-wave propagation in the conduit and transmission to the atmosphere, cannot explain the infrasonic wavefield recorded at Stromboli. Moreover, resonance properties of the magma column is inferred to be responsible not only for the infrasonic waves but also for the seismic wavefield generated by volcanic activity within a frequency range between 1 and 10 Hz, such as tremor. Our results point out that a strong attenuation effect is induced by the bulk and shear viscosity of the gas-rich magma on the acoustic waves just in this frequency range. Our theoretical result on this strong attenuation effect induced by the shear viscosity is partially supported by laboratory experiments on the propagation of shock and pressure waves in high-viscosity liquids (Ichihara et al., 2004). Acoustic resonance in volcanic conduit may occur only when a segment of conduit is dynamically and acoustically stable over at least for few cycles of resonance at the frequency of interest (Lane et al., 2001).

Therefore, we conclude that viscosity changes have a strong attenuation effect on the propagation of viscoelastic waves along a gas-rich magma column and should be more thoroughly considered when resonance is assumed to be a possible mechanisms for the observed acoustic wavefield.

**Acknowledgements**

We are grateful to Bernard Chouet and Jürgen Neuberg for their careful review that greatly improved the manuscript and helped us to clarify the models.

## Appendix A

### *A.1. Formulation of a propagator matrix*

Considering a harmonic field with an angular frequency $\omega$, the displacement $\xi$ and the normal stress $\sigma_{zz}$:

$$\sigma_{zz} = -p + D, \tag{A.1}$$

can both be expressed as:

$$\xi(z,t) = X(z)e^{i\omega t}, \tag{A.2}$$

$$\sigma_{zz} = S(z)e^{i\omega t}. \tag{A.3}$$

The stress–strain vector is defined as:

$$\boldsymbol{B}(z) = [X, \omega^{-1}S]^T. \tag{A.4}$$

According to Eqs. (19), (21) and (15):

$$\frac{\partial \boldsymbol{B}(z)}{\partial z} = \omega \mathbf{A}(z)\boldsymbol{B}(z), \tag{A.5}$$

$$\mathbf{A}(z) = \begin{pmatrix} 0 & (\rho c^2 + i\omega\tfrac{4}{3}\eta_{\text{eff}})^{-1} \\ -\rho + Q_\omega/\omega^2 & 0 \end{pmatrix}. \tag{A.6}$$

To relate the stress–displacement vector (Eq. (A.4)) more directly to the elastic wavefield, the following transformation is made:

$$\boldsymbol{B} = \mathbf{D}\mathbf{V}, \tag{A.7}$$

where $\mathbf{D}$ is the eigenvector matrix for $\mathbf{A}$, that is:

$$\mathbf{A}\mathbf{D} = i\mathbf{D}\Lambda, \tag{A.8}$$

$$\Lambda = \begin{pmatrix} k'/\omega & 0 \\ 0 & -k'/\omega \end{pmatrix}, \tag{A.9}$$

where $k'$ is given by Eq. (30) and $\pm ik'/\omega$ are the eigenvalues of $\boldsymbol{A}$. The explicit form for the matrix $\mathbf{D}$ is:

$$\mathbf{D} = \begin{pmatrix} 1 & 1 \\ i\frac{k'}{\omega}(\rho c^2 + i\omega\frac{4}{3}\eta_{\text{eff}}) & -i\frac{k'}{\omega}(\rho c^2 + i\omega\frac{4}{3}\eta_{\text{eff}}) \end{pmatrix}. \tag{A.10}$$

Within a single uniform layer the new wave vector $\boldsymbol{V}$ then satisfies:

$$\frac{\partial \boldsymbol{V}}{\partial z} = i\omega\Lambda\boldsymbol{V}. \tag{A.11}$$

From Eq. (A.11), one obtains:

$$\boldsymbol{V}(z_{i-1}^+) = \mathbf{E}(z_{i-1}^+, z_i^-)\boldsymbol{V}(z_i^-), \tag{A.12}$$

where the superscripts + and − indicate just beneath and above the boundaries at the depth, respectively. $\mathbf{E}(z_{i-1}^+, z_i^-)$ is a propagator matrix from the bottom to the top of the $i$-th layer ($z_{i-1} < z < z_i$) and given as:

$$\mathbf{E}(z_{i-1}^+, z_i^-) = \begin{pmatrix} e^{ik'(z_{i-1}^+, -z_i^-)} & 0 \\ 0 & e^{-ik'(z_{i-1}^+, -z_i^-)} \end{pmatrix}. \tag{A.13}$$

Then the elements of $\boldsymbol{V}$ may be identified as the amplitudes of upward and downward traveling waves:

$$\boldsymbol{V} = [V_{\text{U}}, V_{\text{D}}]^T. \tag{A.14}$$

Continuity of displacement and stress at $z = z_i$, which is the boundary between $i$-th and $(i+1)$-th boundary requires:

$$\boldsymbol{B}(z_i^-) = \boldsymbol{B}(z_i^+). \tag{A.15}$$

Eq. (A.15) is rewritten using Eq. (A.7) as:

$$\boldsymbol{V}(z_i^-) = \mathbf{D}^{-1}(z_i^-)\mathbf{D}(z_i^+)\boldsymbol{V}(z_i^+), \tag{A.16}$$

where $\mathbf{D}^{-1}(z_i^-)\mathbf{D}(z_i^+)$ is the propagator matrix across the boundary.

Propagation of wavefield from $z=z_j^-$ to $z_i^-$ ($z_j>z_i$) is represented by:

$$\begin{aligned}\boldsymbol{V}(z_i^-) &= \mathbf{D}^{-1}(z_i^-)\mathbf{D}(z_i^+)\mathbf{E}(z_i^+, z_{i+1}^-)\mathbf{D}^{-1}(z_{i+1}^-)\mathbf{D}(z_{i+1}^+) \\ &\quad \times \mathbf{E}(z_{i+1}^+, z_{i+2}^-)\ldots\mathbf{E}(z_{j-1}^+, z_j^-)\boldsymbol{V}(z_j^-), \\ &= \mathbf{Q}(z_i^-, z_j^-)\boldsymbol{V}(z_j^-),\end{aligned} \tag{A.17}$$

where $\mathbf{Q}(z_i^-, z_j^-)$ is defined as a propagator matrix from $z=z_j^-$ to $z_i^-$. In the same way, a propagator matrix from beneath the boundary at $z=z_j$, that is $z=z_j^+$, to $z_i^-$ is represented by:

$$\mathbf{Q}(z_i^-, z_j^+) = \mathbf{Q}(z_i^-, z_j^-)\mathbf{D}^{-1}(z_i^-)\mathbf{D}(z_i^+). \tag{A.18}$$

### A.2. Reflection–transmission coefficients

Reflection and transmission coefficients of a whole layers between $z_i^m$ and $z_j^m$ ($z_i<z_j$) are denoted by $R_{\mathrm{U,D}}(z_i^p, z_j^q)$ and $T_{\mathrm{U,D}}(z_i^p, z_j^q)$, respectively. The superscripts $p$ and $q$ indicate either + or −, which is omitted in the following equations. Wavefield across the boundary is represented in terms of these coefficients as:

$$V_{\mathrm{U}}(z_i) = R_{\mathrm{D}}(z_i, z_j)V_{\mathrm{D}}(z_i) + T_{\mathrm{U}}(z_i, z_j)V_{\mathrm{U}}(z_j), \tag{A.19}$$

$$V_{\mathrm{D}}(z_j) = T_{\mathrm{D}}(z_i, z_j)V_{\mathrm{D}}(z_i) + R_{\mathrm{U}}(z_i, z_j)V_{\mathrm{U}}(z_j), \tag{A.20}$$

While Eq. (A.17) is expanded representing elements of $\boldsymbol{Q}$ by $q_{ij}$:

$$V_{\mathrm{U}}(z_i) = q_{11}(z_i, z_j)V_{\mathrm{U}}(z_j) + q_{12}(z_i, z_j)V_{\mathrm{D}}(z_j), \tag{A.21}$$

$$V_{\mathrm{D}}(z_i) = q_{21}(z_i, z_j)V_{\mathrm{U}}(z_j) + q_{22}(z_i, z_j)V_{\mathrm{D}}(z_j), \tag{A.22}$$

Comparing Eqs. (A.19), (A.20) and (A.21), (A.22), the following relations are obtained:

$$\left.\begin{aligned} T_{\mathrm{D}} &= q_{22}^{-1} \\ R_{\mathrm{D}} &= q_{12}q_{22}^{-1} \\ T_{\mathrm{U}} &= q_{11} - q_{12}q_{22}^{-1}q_{21} \\ R_{\mathrm{U}} &= -q_{22}^{-1}q_{21} \end{aligned}\right\} \tag{A.23}$$

### A.3. Wave transmission into a half space

We are interested in wave transmission from a source in the magma ($z=z_s^-$) to the air ($z=z_0^-$). Because the air is regarded as an infinite half space and we do not assume pressure source in the air, there is no downward wave in the air ($V_{\mathrm{D}}(z_0^-)=0$). From Eq. (A.19) with $z_i=z_0^-$ and $z_j=z_s^-$, we have:

$$V_{\mathrm{U}}(z_0^-) = T_{\mathrm{U}}(z_0^-, z_s^-)V_{\mathrm{U}}(z_s^-). \tag{A.24}$$

The stress–displacement vector in the air ($z_0^-$) and in the magma at $z_s^-$ associated with the upward waves, $V_{\mathrm{U}}(z_0^-)$ and $V_{\mathrm{U}}(z_s^-)$ are then calculated by:

$$\begin{aligned}\boldsymbol{B}(z_0^-) &= \mathbf{D}(z_0^-)\begin{pmatrix} V_{\mathrm{U}}(z_0^-) \\ \\ 0 \end{pmatrix} \\ &= \begin{pmatrix} 1 \\ \\ i\rho_0 c_0 \end{pmatrix} T_{\mathrm{U}}(z_0^-, z_s^-)V_{\mathrm{U}}(z_s^-),\end{aligned} \tag{A.25}$$

$$\begin{aligned}\boldsymbol{B}(z_s^-) &= \mathbf{D}(z_s^-)\begin{pmatrix} V_{\mathrm{U}}(z_s^-) \\ \\ 0 \end{pmatrix} \\ &= \begin{pmatrix} 1 \\ \\ ik_{\mathrm{s}}'\ \omega^{-1}(\rho_{\mathrm{s}}c_{\mathrm{s}}^2 + i\omega\tfrac{4}{3}\eta_{\mathrm{eff,s}}) \end{pmatrix} V_{\mathrm{U}}(z_s^-),\end{aligned} \tag{A.26}$$

where material parameters for air and in the $s$-th layer are indicated by subscripts 0 and $s$, respectively.

From Eqs. (A.3) and (A.4), the corresponding normal stresses are:

$$\sigma_{zz}(z_0^-) = i\omega\rho_0 c_0 T_{\mathrm{U}}(z_0^-, z_s^-) V_{\mathrm{U}}(z_s^-) e^{i\omega t}, \tag{A.27}$$

$$\sigma_{zz}(z_s^-) = ik_{\mathrm{s}}' \left(\rho_{\mathrm{s}} c_{\mathrm{s}}^2 + i\omega \frac{4}{3}\eta_{\mathrm{eff,s}}\right) V_{\mathrm{U}}(z_s^-) e^{i\omega t}, \tag{A.28}$$

According to Eqs. (19), (21) and (A.1), the relation between the pressure ($p$) and the normal stress ($s_{zz}$) is:

$$\frac{p}{\sigma_{zz}} = \frac{\rho c^2 + i\omega\eta_{\mathrm{b}}}{\rho c^2 + i\omega\frac{4}{3}\eta_{\mathrm{eff}}} \tag{A.29}$$

The ratio of pressure amplitude at $z_s^-$ to that at $z_0^-$ is then given as:

$$\left|\frac{p_{\mathrm{source}}}{p_{\mathrm{air}}}\right| = \left|\frac{k_{\mathrm{s}}'}{\omega} \frac{\rho_{\mathrm{s}} c_s^2 + i\omega\eta_{\mathrm{b}}}{\rho_0 c_0 T_{\mathrm{U}}(z_0^-, z_s^-)}\right|. \tag{A.30}$$

## References


Achard, J.L., Lespinard, G.M., 1981. Structure of the transient wall-friction law in one-dimensional models of laminar pipe flows. J. Fluid Mech. 113, 283–298.

Aki, K., Chouet, B., Fehler, M., Zandt, G., Koyanagi, R., Colp, J., Hay, R.G., 1978. Seismic properties of a shallow magma reservoir in Kilauea Iki by active and passive experiments. J. Geophys. Res. 83, 2273–2282.

Allard, P., Carbonnelle, J., Metrich, N., Loyer, H., Zettwoog, P., 1994. Sulfur output and magma degassing budget of Stromboli Volcano. Nature 368, 326–330.

Bagdassarov, N.S., Dingwell, D.B., 1993. Frequency dependent rheology of vesicular rhyolite. J. Geophys. Res. 98, 6477–6487.

Buckingham, M.J., Garces, M.A., 1996. Canonical model of volcano acoustics. J. Geophys. Res. 101, 8129–8151.

Cashman, K.V., Mangan, M.T., 1994. Physical aspects of magmatic degassing: 2. Constraints on vesiculation processes from textural studies of eruptive products. In: Carrol, M.R., Holloway, J.R. (Eds.), Volatiles in Magmas. Rev. Mineral., 30, 413–443.

Chouet, B., 1985. Excitation of a buried magmatic pipe—a seismic source model for volcanic tremor. J. Geophys. Res. 90, 1881–1893.

Chouet, B., 1996. New methods and future trends in seismological volcano monitoring. In: Scarpa, R., Tilling, R.I. (Eds.), Monitoring and Mitigation of Volcano Hazards. Springer-Verlag, Berlin, pp. 23–97.

Chouet, B., Dawson, P., Ohminato, T., Martini, M., Saccorotti, G., Giudicepietro, F., De Luca, G., Milana, G., Scarpa, R., 2003. Source mechanisms of explosions at Stromboli Volcano, Italy, determined from moment-tensor inversions of very-long-period data. J. Geophys. Res. 108, 2019 (doi:10.1029/2002JB001919).

Commander, K.W., Prosperetti, A., 1989. Linear pressure waves in bubbly liquids: comparison between theory and experiments. J. Acoust. Soc. Am. 85, 732–746.

Dingwell, D.B., Webb, S.L., 1989. Structural relaxation in silicate melts and non-Newtonian melt rheology in geologic processes. Phys. Chem. Miner. 16, 508–516.

Dobran, F., 1992. Nonequilibrium-flow in volcanic conduits and application to the eruptions of Mt. St.-Hellens on May 18, 1980, and Vesuvius in A.D. 79. J. Volcanol. Geotherm. Res. 49, 285–311.

Francalanci, L., Taylor, S.R., Mcculloch, M.T., Woodhead, J.D., 1993. Geochemical and isotopic variations in the calc-alkaline rocks of Aeolian Arc, Southern Tyrrhenian Sea, Italy—constraints on magma genesis. Contrib. Mineral. Petrol. 113, 300–313.

Garces, M.A., 1997. On the volcanic waveguide. J. Geophys. Res. 102 (B10), 22547–22564.

Garces, M., McNutt, S.R., Hansen, R.A., Eichelberger, J.C., 2000. Application of wave-theoretical seismoacoustic models to the interpretation of explosion and eruption tremor signals radiated by Pavlof volcano, Alaska. J. Geophys. Res. 105, 3039–3058.

Gibson, F.W., 1970. Measurements of the effect of air bubbles on the speed of sound in water. J. Acoust. Soc. Am. 48, 1195–1197.

Hamilton, D.L., Burnham, C.W., Osborn, E.F., 1964. The solubility of water and effects of oxygen fugacity and water content on crystallization in mafic magmas. J. Petrol. 5, 21–39.

Ichihara, M., Kameda, M., 2004. Propagation of acoustic waves in a visco-elastic two-phase system: Influence of the liquid viscosity and the internal diffusion. J. Volcanol. Geotherm. Res. doi: 10.1016/j.volgeores.2004.05.001.

Ichihara, M., Ohkunitani, H., Ida, Y., Kameda, M., 2004. Dynamics of bubble oscillation and wave propagation in viscoelastic liquids. J. Volcanol. Geotherm. Res. 129, 37–60.

Jaupart, C., 1996. Physical models of volcanic eruptions. Chem. Geol. 128, 217–227.

Jaupart, C., Vergniolle, S., 1989. The flow of gas and lava—a review of dynamic-models for volcanic-eruptions. Chem. Geol. 70, 38.

Johnson, J.B., Aster, R.C., Ruiz, M.C., Malone, S.D., McChesney, P.J., Lees, J.M., Kyle, P.R., 2003. Interpretation and utility of infrasonic records from erupting volcanoes. J. Volcanol. Geotherm. Res. 121, 15–63.

Julian, B.R., 1994. Volcanic tremor: nonlinear excitation by fluid flow. J. Geophys. Res. 99, 11859–11877.

Kazahaya, K., Shinohara, H., Saito, G., 1994. Excessive degassing of Izu-Oshima volcano-magma convection in a conduit. Bull. Volcanol. 56, 207–216.

Kennet, L.N., Kerry, N.J., 1979. Seismic waves in a stratified half space. Geophys. J. R. Astron. Soc. 57, 557–583.

Kieffer, S.W., 1977. Sound speed in liquid–gas mixtures: water–air and water–steam. J. Geophys. Res. 82, 2895–2904.

Kinsler, L.E., Frey, A.R., 1962. Fundamentals of Acoustics. Wiley and Sons, New York.

Landau, L.D., Lifshitz, E.M. (Eds.), 1987. Fluid Mechanics, 2nd. Ed. Pergamon Press, Oxford.

Lane, S.J., Chouet, B.A., Phillips, J.C., Dawson, P., Ryan, G., Hurst, E., 2001. Experimental observations of pressure oscillations and flow regimes in an analogue volcanic system. J. Geophys. Res. 106, 6461–6476.

Lyakhovsky, V., Hurwitz, S., Navon, O., 1996. Bubble growth in rhyolitic melts: experimental and numerical investigation. Bull. Volcanol. 58, 19–32.

Massol, H., Jaupart, C., 1999. The generation of gas overpressure in volcanic eruptions. Earth Planet. Sci. Lett. 166, 57–70.

Melnik, O., Sparks, R.S.J., 1999. Nonlinear dynamics of lava dome extrusion. Nature 402, 37–41.

Murase, T., McBirney, R., 1973. Properties of some common igneous rocks and their melt at high temperature. Geol. Soc. Amer. Bull. 84, 3563–3592.

Navon, O., Chekhmir, A., Lyakhovsky, V., 1998. Bubble growth in highly viscous melts: theory, experiments, and autoexplosivity of dome lavas. Earth Planet. Sci. Lett. 160, 763–776.

Neuberg, J., 2000. Characteristics and causes of shallow seismicity in andesite volcanoes. In: Francis, P., Neuberg, J., Sparks, R.S.J. (Eds.), The causes and consequences of eruptions of andesite volcanoes. Philos. Trans. R. Soc. 358, 1533–1546.

Neuberg, J., Luckett, R., Baptie, B., Olsen, K.B., 2000. Models of tremor and low-frequency earthquake swarms on Montserrat. J. Volcanol. Geotherm. Res. 101, 83–104.

Pineau, F., Javoy, M., 1994. Strong degassing at ridge crests: the behaviour of dissolved carbon and water in basalt glasses at 14(tm)-N, Mid-Atlantic Ridge. Earth Planet. Sci. Lett. 123, 179–198.

Prosperetti, A., 1984. Bubble phenomena in sound fields 2. Ultrasonics 22, 115–124.

Proussevitch, A.A., Sahagian, D.L., Kutolin, V.A., 1993. Stability of foams in silicate melts. J. Volcanol. Geotherm. Res. 59, 161–178.

Richet, P., Lejeune, A., Holtz, F., Roux, J., 1996. Water and the viscosity of andesite melts. Chem. Geol. 128, 185–197.

Ripepe, M., Gordeev, E., 1999. Gas bubble dynamics model for shallow volcanic tremor at Stromboli. J. Geophys. Res. 104, 10639–10654.

Ripepe, M., Marchetti, E., 2002. Array tracking of infrasonic sources at Stromboli Volcano. Geophys. Res. Lett. 29, 2076 (doi:10.1029/2002GL015452).

Ripepe, M., Poggi, P., Braun, T., Gordeev, E., 1996. Infrasonic waves and volcanic tremor at Stromboli. Geophys. Res. Lett. 23, 181–184.

Ripepe, M., Ciliberto, S., Della Schiava, M., 2001a. Time constraints for modeling source dynamics of volcanic explosions at Stromboli. J. Geophys. Res. 106, 8713–8727.

Ripepe, M., Coltelli, M., Gresta, S., Moretti, M., Piccinini, D., Privitera, E., 2001b. Seismic and infrasonic evidence for an impulsive source of shallow volcanic tremor at Mt. Etna, Italy. Geophys. Res. Lett. 28, 1071–1074.

Saar, M.O., Manga, M., Cashman, K.V., Fremouw, S., 2001. Numerical models of the onset of yield strength in crystal-melt suspensions. Earth Planet. Sci. Lett. 187, 367–379.

Shaw, H.R., 1972. Viscosities of magmatic silicate liquids: an empirical method of prediction. Am. J. Sci. 272, 870–893.

Sparks, R.S.J., 1978. The dynamics of bubble formation and growth in magmas: a review and analysis. J. Volcanol. Geotherm. Res. 28, 257–274.

Sparks, R.S.J., Barkley, J., Jaupart, C., Mader, H.M., Phillips, J.C., 1994. Physical aspects of magmatic degassing: I. Experimental and theoretical constraints on vesiculation. In: Carrol, M.R., Holloway, J.R. (Eds.), Volatiles in Magmas. Rev. Mineral., 30, 413–445.

Spera, F.J., 1999. Physical properties of magmas. In: Sigurdsson, H.B., Houghton, H.B., McNutt, S.R., Rymer, H., Stix, J. (Eds.), Encyclopedia of Volcanoes. Academic Press, San Diego, pp. 171–190.

Stein, D.J., Spera, F.J., 1992. Rheology and microstructure of magmatic emulsions: theory and experiments. J. Volcanol. Geotherm. Res. 49, 157–174.

Stevenson, D.S., Blake, S., 1998. Modelling the dynamics and thermodynamics of volcanic degassing. Bull. Volcanol. 60, 307–317.

Stolper, E., Holloway, J.R., 1988. Experimental determination of the solubility of carbon dioxide in molten basalt at low pressure. Earth Planet. Sci. Lett. 87, 397–408.

Tait, S., Jaupart, C., Vergniolle, S., 1989. Pressure, gas content and eruption periodicity of a shallow, crystallising magma chamber. Earth Planet. Sci. Lett. 92, 107–123.

Toramaru, A., 1989. Vesiculation process and bubble-size distributions in ascending magmas with constant velocities. J. Geophys. Res. 94, 17523–17542.

Vergniolle, S., Brandeis, G., 1996. Strombolian explosions: 1. A large bubble breaking at the surface of a lava column as a source of sound. J. Geophys. Res. 101, 20433–20447.

Vergniolle, S., Brandeis, G., Marechal, J.C., 1996. Strombolian explosions: 2. Eruption dynamics determined from acoustic measurements. J. Geophys. Res. 101, 20449–20466.

Webb, S.L., 1997. Silicate melts: Relaxation, rheology, and glass transition. Rev. Geophys. 35, 191–218.

Yoshida, S., Koyaguchi, T., 1999. A new regime of volcanic eruption due to the relative motion between liquid and gas. J. Volcanol. Geotherm. Res. 89, 303–315.